ELSEVIER

Thermochimica Acta 287 (1996) 191–201

thermochimica acta

Enthalpy, heat capacity, second-order transitions and enthalpyof fusion of Li_4SiO_4 by high-temperature calorimetry[1]

H. Kleykamp

Forschungszentrum Karlsruhe, Institut für Materialforschung I, Postfach 3640, 76021 Karlsruhe, Germany

Received 19 December 1995; accepted 29 March 1996

Abstract

The enthalpy of Li_4SiO_4 was obtained between 363 and 1300 K using isothermal drop calorimetry. Anisothermal calorimetry was used for the identification of two second-order transitions and the measurement of the enthalpy of fusion. The smoothed enthalpy between 298 and 1300 K results in $H°(T) - H°(298) = -17156 + 73.694\ T + 0.103210\ T^2 - 4163115\ T^{-1}$ J mol^{-1}. The heat capacity was derived by differentiation. The value extrapolated to 298 K is $C_{p,298} = 182.1$ J K^{-1} mol^{-1}. The critical temperatures of the second-order transitions are $T_{c1} = 938$ K and $T_{c2} = 996$ K. The enthalpy of fusion is $\Delta_{fus}H = 53$ kJ mol^{-1} at the melting temperature $T_m = 1531$ K. An isotope effect of the ^{6}Li enrichment on the melting temperature and enthalpy of fusion could not be discerned.

Keywords: Enthalpy; Enthalpy of fusion; Heat capacity; Li_4SiO_4; Second-order transition

1. Introduction

Lithium orthosilicate is being considered as a possible solid breeder material in the blanket of future fusion reactors. The role of the material is to produce tritium atoms, which act as fuel components of the reactor. As the heat generated by this nuclear fusion reaction is absorbed by the blanket and transferred to the coolant, the thermal properties, such as the enthalpy, heat capacity and transition temperatures, and the structural integrity of the breeder materials are of primary importance for the design of a blanket system.

[1] The paper was presented partly at 11. Ulmer Kalorimetrietage, Freiberg/Sa., 29–31 March 1995.

PII: S0040-6031(96)02996-6

1.1. Literature survey

Lithium orthosilicate is a line compound with a congruent melting temperature at 1255°C [1]. The phase crystallizes at room temperature in a monoclinic structure [2–6]. A phase transition into a pseudo-orthorhombic structure is assumed to take place at 666°C [7, 8, 9]. Three transitions were observed by differential thermal analysis (DTA) during heating at 610, 660 and 725°C [10] and at 600, 665 and 725°C [11], respectively. High-temperature X-ray diffraction of Li_4SiO_4 between room temperature and 900°C showed no discontinuity of the lattice parameters except for a slight decrease in the *c*-axis between 600 and 800°C followed by a further increase above this temperature [1, 6]. The transition observed at 665°C by differential scanning calorimetry (DSC) was recognized to be reversible and displacive [6]; a transition was also reported to be at 672°C [12].

The heat capacity of Li_4SiO_4 was measured by DSC between room temperature and 470°C [13] and between room temperature and 630°C [12]. The enthalpy was calculated by integration of the heat capacity. The enthalpy of Li_4SiO_4 was also obtained by drop calorimetry between room temperature and 730°C. The heat capacity was calculated by differentiation of the enthalpy using a modified quasi-local linear regression method. Three humps were observed at 612, 657 and 712°C [14]. Furthermore, the heat capacity and the enthalpy of Li_4SiO_4 were estimated in an assessment [15].

1.2. Second-order transitions

A second-order transition proceeds steadily in a temperature region by uptake of additional heat from the surroundings for the generation of disorder. This is connected with a finite increase of the heat capacity C_p up to a maximum value at the critical temperature T_c. Enthalpy and entropy remain continuous and differentiable functions in this temperature region whereas the heat capacity is continuous but not differentiable. The disordered fraction of C_p above the basic $C_p(T)$ curve, δC_p, can be calculated by introduction of an order parameter, attaining a maximum value of $\delta C_p = 3\,R/2$ at T_c [16]. C_p should drop back steeply to the basic $C_p\,(T)$ curve above T_c. In this temperature region, however, some short-range order remains which is expressed in the $C_p(T)$ curve by a slow decrease due to further heat consumption for the destruction of the residual short-range order above T_c. There is no two-phase equilibrium at the critical temperature.

The enthalpy and entropy of transition are zero for a second-order transition. Nevertheless, a signal develops by DTA which is based on an additional heat flow from the surroundings in the heating mode. The signal increases steadily up to T_c and differs distinctly from the signal of a first-order transition. The different peak shapes and the reversible behaviour are illustrated in Fig. 1 for cobalt with a first-order structural hcp→fcc transition at 422°C and a second-order ferromagnetic–paramagnetic transition at 1121°C.

Selected second-order transitions are compiled in Table 1 [17–23]. The order–disorder transition of $AuCu_3$ is first order, because the order parameter S decreases discontinuously for $S \leq 0.46$ to zero; furthermore, the ferroelectric–paraelectric transi-

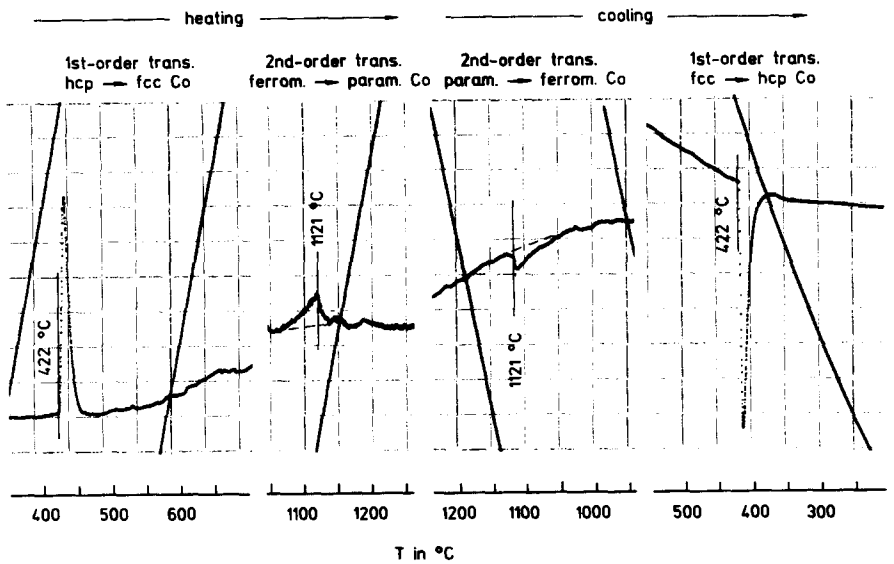

Fig. 1. First-order and second-order transitions of cobalt identified by different peak shapes of the DTA signal.

Table 1
Critical temperatures T_c and heat capacities δC_p^a of selected second-order transitions

Phase	Transition	T_c/K	δC_p/J K^{-1} g-atom^{-1}	Ref.
β'-β brass	Order–disorder	742	40	[17]
AuCuI–AuCuII	Order–disorder	658	≃25	[18]
US	Ferromagn.–paramagn.	180	21	[19]
α-Fe	Ferromagn.–paramagn.	1043	≃35	[18]
α-Co	Ferromagn.–paramagn.	1394	≃15	[18]
$Fe_{0.95}O$	Antiferromagn.–paramagn.	189	8	[20]
$(NH_2CH_2COOH)_3 \cdot H_2SO_4$	Ferroelectric–paraelectric	322	≃5	[21]
$NaNO_2$	Antiferroelectric–paraelectric	438	20	[22]
Sn	Supercon.–normal cond. (magnetic field H=O)	3.7	0.011	[23]

[a] δC_p is the maximum $C_p$value above the basic $C_p(T)$ curve at T_c.

tion of $BaTiO_3$ is also first order because the electric transition is coupled with the structural tetragonal–cubic transition.

2. Experimental

2.1. Materials

A stoichiometric Li_4SiO_4 melt was air-sprayed between 1350 and 1400°C by Schott Glaswerke, Mainz, to form single-phase granules up to 1 mm in diameter. This method

involves rapid quenching and possibly internal stress and glass formation. The material was granulated, re-compacted and annealed at 900°C for 10 min in dry air to relieve stresses, to attain complete recrystallization and to remove adsorbed H_2O and CO_2 immediately before the X-ray diffraction and calorimetric measurements. X-ray diffraction was carried out at room temperature by the Guinier method with $CuK\alpha_1$ radiation ($\lambda = 154.060$ pm) and calibration with an internal NaCl standard ($a = 564.02$ pm). The positions of the diffraction lines were determined with a Huber comparator; the intensities were estimated by visual inspection. Fourteen lines of the X-ray diffraction pattern listed in Table 2 were evaluated. The material is single-phase. The lattice parameters were calculated by an optimization programme which results in $a = (529.6 \pm 0.2)$ pm, $b = (611.0 \pm 0.3)$ pm, $c = (514.5 \pm 0.2)$ pm, $\beta = (90.27 \pm 0.05)°$. Two formula units form the elementary cell. The X-ray density was calculated to $\rho_x = 2.391\ \mathrm{Mg\ m^{-3}}$.

2.2. Calorimetry

The enthalpy measurements of Li_4SiO_4 specimens in the 100 mg range were carried out in the isothermal mode of the high-temperature calorimeter HTC 1800 (Setaram S.A., Lyon, France) between 90 and 1027°C by dropping the specimens at 25°C into the preheated working cell. The transition temperatures and the integrals of the excess heat capacities were determined in the anisothermal mode by heating the samples at a rate of $2\ \mathrm{K\ min^{-1}}$ from room temperature up to about 800°C. The sensitivity factor of the calorimeter was determined with the known enthalpy of α-Al_2O_3. Details of the calibration are described in Ref. [24]. Platinum liners were used inside the working and reference Al_2O_3 crucibles in these experiments in order to reduce the standard deviation of calibration and measurement. This was achieved by a more uniform heat flux through the crucible walls. The enthalpy of fusion of Li_4SiO_4 was measured in the

Table 2
X-ray diffraction pattern of Li_4SiO_4 at room temperature

hkl	d_{obs}/pm	Rel. intensity	d_{calc}/pm
100	528.3	m.	529.55
001	513.3	w.	514.54
110	400.1	v. st.	400.17
011	393.5	st.	393.57
101	368.2	m.	368.15
−111	316.4	m.	316.44
020	305.1	w.	305.50
002	257.4	st.	257.27
210	243.1	w.	242.94
211	219.3	w.	219.32
−221	186.7	w.	186.71
301	166.7	w.	166.72
231	154.0	w.	153.90
023	149.6	w.	149.56

cooling mode of the calorimeter at a rate of $-0.5\,K\,min^{-1}$ without platinum liners in order to avoid chemical reactions with the melts. The sensitivity factor was determined with the known enthalpy of solidification of gold and nickel [15] and by linear interpolation to the actual solidification temperatures of the Li_4SiO_4 samples. The measurement of the enthalpy of solidification was preferred to that of the enthalpy of fusion because the onset temperature was difficult to determine in the latter case. An undercooling of between 5 and 20 K was observed at the cooling rate of $-0.5\,K\,min^{-1}$ of the calorimeter. The temperatures were calibrated by the melting temperatures of In, Sn, Zn, Al, Ag, Au and Ni. Enthalpy and solid transition temperature measurements were performed with unprotected specimens; melting temperature and enthalpy of fusion measurements were made with samples that were sealed with platinum foils in order to reduce vaporization effects. The occurrence of any isotope effect of $^6Li/^7Li$ on the melting temperature and the enthalpy of fusion of Li_4SiO_4 was studied using Li-nat (7.5% ^6Li) and enriched (50% ^6Li) materials.

3. Results

3.1. Second-order transitions, melting temperature and enthalpy of fusion

Preliminary experiments by DTA have shown two peaks at around 660 and 720°C which were attributed to transitions of Li_4SiO_4. These peaks were also observed in the literature [10, 11, 14]. However, the third peak formed at around 610°C [10, 11, 14] could not be confirmed in this work on Li_4SiO_4 that had been heat-treated at 900°C for 10 min before the measurements. Therefore, this peak could be associated with recrystallization and adsorption effects.

Detailed analysis by DTA and calorimetry revealed peak shapes that are similar to those of the ferromagnetic–paramagnetic transition of cobalt in Fig. 1. The heat flow curves by anisothermal calorimetry in the temperature range of the second-order transitions of Li_4SiO_4 are illustrated in Fig. 2. The peaks are explained by second-order transitions. This is supported by the absence of a discontinuity in the high-temperature lattice parameters [1, 6]. The endothermal peaks develop gradually during heating. The first peak starts at 648°C, passes a maximum at 665°C, vanishes at 683°C and corresponds to an integrated heat flow of $900\,J\,mol^{-1}$. Hence

$$\int_{648}^{683} \delta C_p \, d\theta = 900\,J\,mol^{-1}$$

If the integral can be approximated by a saw-toothed function $1/2\,\delta C_{p,max}\,\Delta T$, then $\delta C_{p,max} = 51\,J\,K^{-1}\,mol^{-1}$ Li_4SiO_4 is obtained. The second peak starts at 713°C, passes a maximum at 723°C, vanishes at 735°C and corresponds to an integrated heat flow of $630\,J\,mol^{-1}$. Hence

$$\int_{713}^{735} \delta C_p \, d\theta = 630\,J\,mol^{-1}$$

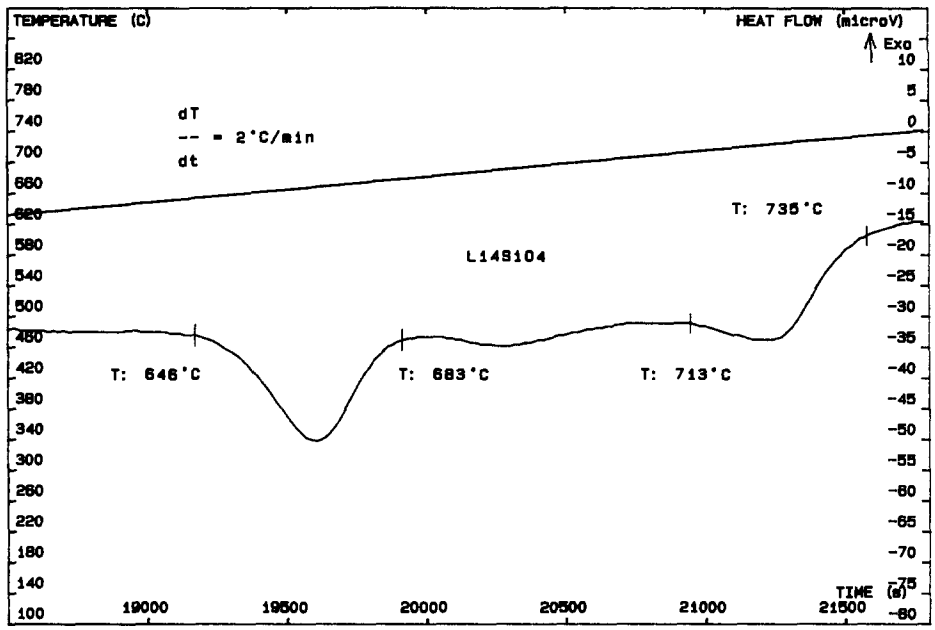

Fig. 2. Second-order transitions of Li_4SiO_4 identified by the heat flow curve of the calorimeter.

This results in $\delta C_{p,max} = 57\,J\,K^{-1}\,mol^{-1}$ Li_4SiO_4. The peak maxima are located at the critical temperatures $T_{c1} = 665°C$ and $T_{c2} = 723°C$.

The melting temperature and the enthalpy of fusion of Li_4SiO_4 were determined on Li_4SiO_4 samples in the 250 mg range with $^6Li/Li\text{-total} = 0.075$ and $^6Li/Li\text{-total} = 0.50$. The samples were encapsulated in platinum foils in order to reduce the Li_2O evaporation during heating above 1000°C. The same amount of platinum foil was placed in the reference crucible of the calorimeter. The melting temperature of Li_4SiO_4 is $T_m = (1258 \pm 1)°C$ [25]. An isotope effect was not noticed. The sensitivity factors S_T of the calorimeter were obtained by five measurements, of the heat flux of the enthalpies of solidification of gold, $\Delta_{sol}H = -12552\,J\,mol^{-1}$ at $T_m = 1064°C$, and of nickel, $\Delta_{sol}H = -17472\,J\,mol^{-1}$ at $T_m = 1455°C$, which result in $S_{1337} = (0.615 \pm 0.019)\,\mu V\,mW^{-1}$ and $S_{1728} = (0.353 \pm 0.012)\,\mu V\,mW^{-1}$. The linear interpolation to the melting temperature of Li_4SiO_4 at 1258°C gives $S_{1531} = (0.485 \pm 0.022)\,\mu V\,mW^{-1}$. The heat flux measurements of Li_4SiO_4 during solidification at 5–20 K below the melting temperature and the sensitivity factors at the actual solidification temperatures result in the enthalpy of fusion of Li_4SiO_4 of $\Delta_{fus}H = +(53 \pm 4)\,kJ\,mol^{-1}$. An isotope effect was not noticed.

3.2. Enthalpy and heat capacity

The enthalpy $H°(T) - H°(298)$ of Li_4SiO_4 was measured in the isothermal mode between 363 and 1300 K. Mass losses up to 0.5% were observed after the experi-

ment above the selected temperature range. The anisothermal investigations had shown that the local increase of the enthalpy in the temperature region of the second-order transitions is small compared to the enthalpy and its standard deviation. Therefore, a smoothed curve of the experimental points presented in Table 3 was fitted to a polynomial $H^\circ(T) - H^\circ(298) = a + b\,T + c\,T^2 + d\,T^{-1}$ by the least-squares method which gives $H^\circ(T) - H^\circ(298) = -17156 + 73.6936\,T + 0.103210\,T^2 - 4163115\,T^{-1}$ J mol^{-1} between 298 and 1300 K, see Fig. 3. The 68% standard deviation of the experimental data is 3%. The enthalpy is given numerically in 100 K

Table 3
Experimental results of the enthalpy of Li_4SiO_4

T/K	$H^\circ(T) - H^\circ(298)$/J mol^{-1}		Deviation/%
	Exp.	Calc.	
363	10750	11726	−9.1
396	19124	17699	7.5
440	27925	25789	7.7
493	36395	35816	1.6
548	45306	46626	−2.9
574	52906	51897	1.9
596	57598	56443	2.0
605	59894	58326	2.6
643	63846	66427	−4.0
683	74204	75229	−1.4
721	82825	83857	−1.3
765	91748	94180	−2.7
793	100447	100938	−0.5
818	103457	107098	−3.5
848	112768	114647	−1.7
872	117994	120812	−2.4
893	124078	126297	−1.8
919	129247	133208	−3.1
948	141042	141072	−0.0
962	149690	144927	3.2
971	151232	147426	2.5
999	158583	155303	2.1
1022	166852	161889	3.0
1047	175000	169168	3.3
1069	175657	175675	−0.0
1105	192008	186533	2.9
1127	199433	193296	3.1
1158	204778	202991	0.9
1170	201664	206795	−2.5
1187	214010	212234	0.8
1200	220495	216433	1.8
1221	220012	223288	−1.5
1250	227450	232900	−2.4
1269	237009	239290	−1.0
1300	246234	249873	−1.5

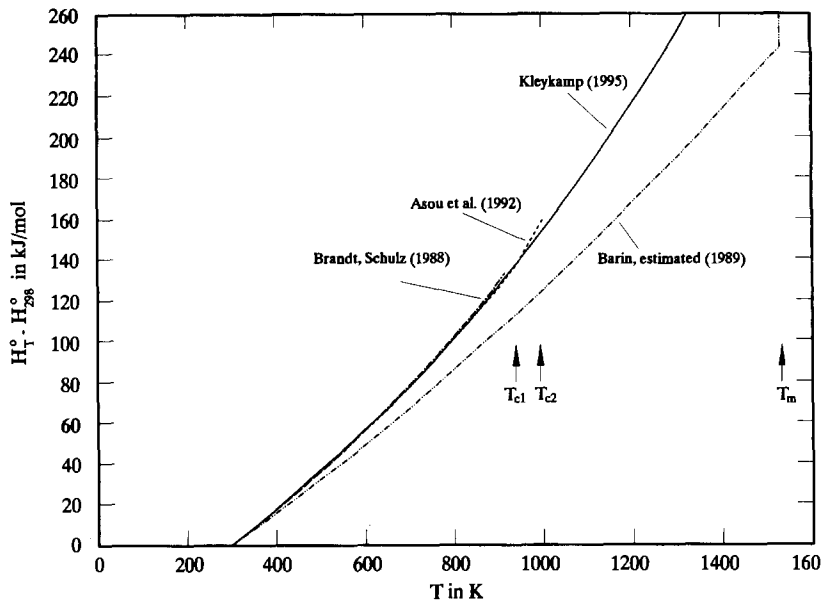

Fig. 3. Enthalpy $H^\circ(T) - H^\circ(298)$ of Li_4SiO_4 as a function of temperature.

intervals in Table 4. The heat capacity C_p of Li_4SiO_4 was evaluated by differentiation of the enthalpy polynomial which results in $C_p(T) = 73.6936 + 0.206420\,T + 4163115\,T^{-1}\,J\,K^{-1}\,mol^{-1}$ between 298 and 1300 K, see Fig. 4. The heat capacity is given numerically in 100 K intervals in Table 5. The value at 298 K is $C_p(298) = (182.1 \pm 5.4)\,J\,K^{-1}\,mol^{-1}$. It should be noted that this result is obtained by an extrapolation from the experimental temperature range above 363 K. It is problematic to deduce heat capacity data in a second-order temperature region from enthalpy data measured by drop calorimetry. Therefore, the heat capacity of Li_4SiO_4 is not presented in the temperature range 910–1020 K in Fig. 4 and Table 5.

4. Discussion

Two transitions were observed in Li_4SiO_4 at $T_{c1} = 665°C$ and $T_{c2} = 723°C$ which are interpreted as second-order type based on the peak shapes and the gradual heat consumption from the surroundings. The nature of the second-order transitions was not investigated further. Li_4SiO_4 melts congruently at 1258°C; an isotope effect of $^6Li/^7Li$ on the melting temperature was not observed. The experimental value is slightly higher compared to previous results [1, 15]. The enthalpy of Li_4SiO_4 has been measured by Asou et al. [14] by drop calorimetry up to 1000 K, and the heat capacity evaluated from this by a modified quasi-local linear regression method. The heat capacity of Li_4SiO_4 was determined by DSC by Brandt and Schulz up to 900 K [12] and by Hollenberg and Baker up to 750 K [13]; the enthalpy was calculated by integration of the heat capacity. The thermal data of these authors [12–14] compiled in

Table 4
Enthalpy $H°(T)-H°(298)$ of Li_4SiO_4

T/K	$H°(T)-H°(298)$/J mol^{-1}			
	Ref. [15]	Ref. [12]	Ref. [14]	This study
298	0	0	0	0
300	272	327	288	364
400	15575	17356	17268	18427
500	31890	35980	36343	37168
600	49052	56379	56990	57278
700	66991	78630	78985	79056
800	85672	102771	102215	102651
900	105075	128825	(124923)	128145
1000	125188	–	(159687)	155587
1100	146005	–	–	185010
1200	167520	–	–	216433
1300	189729	–	–	249873
1400	212631	–	–	(285338)
1500	236223	–	–	–
Method	Assessment	DSC	Drop cal.	Drop cal.

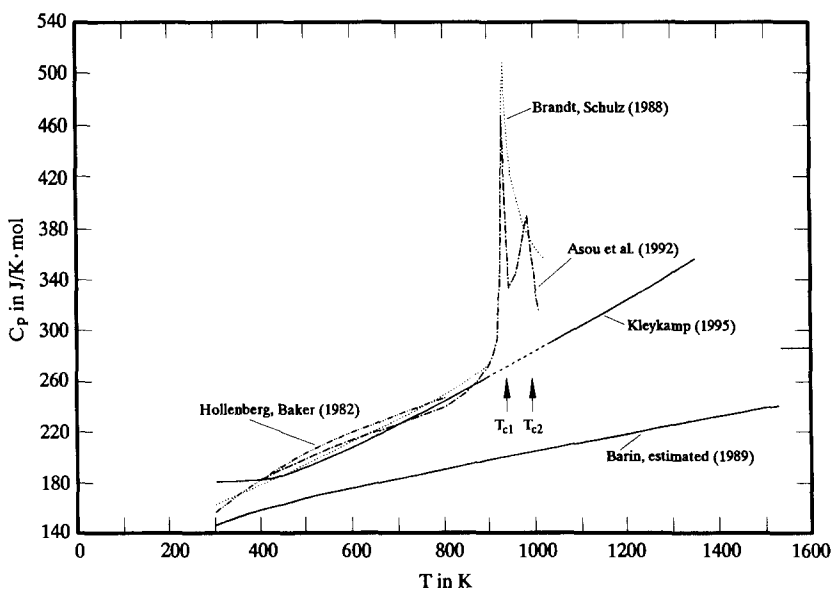

Fig. 4. Heat capacity C_p of Li_4SiO_4 as a function of temperature.

Table 5
Heat capacity C_p of Li_4SiO_4

T/K	C_p/J K^{-1} mol^{-1}				
	Ref. [15]	Ref. [13][a]	Ref. [12]	Ref. [14]	This study
298	146.6	156	163.3	155.2	182.1
300	146.9	156	163.5	155.8	181.9
400	158.5	182	177.8	181.6	182.3
500	167.5	203	194.9	199.1	193.6
600	175.6	219	213.2	213.4	209.1
700	183.1	234	231.9	226.2	226.7
800	190.4	(247)	251.0	238.2	245.3
900	197.6	–	270.2	(274.2)	264.6
1000	204.7	–	–	(358.6)	–
1100	211.7	–	–	–	304.2
1200	218.6	–	–	–	324.3
1300	225.6	–	–	–	344.5
1400	232.5	–	–	–	(364.8)
1500	239.4	–	–	–	–
Method	Assessment	DSC	DSC	Drop cal.	Drop cal.

[a] Data taken from the graph.

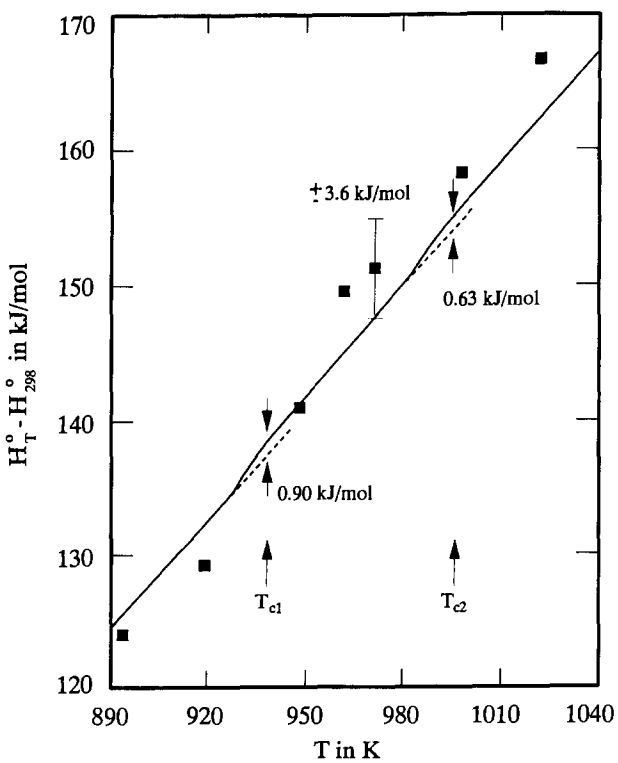

Fig. 5. Enthalpy $H°(T) - H°(298)$ of Li_4SiO_4 in the region of the second-order transitions.

Tables 4 and 5 agree well with the enthalpy and heat capacity obtained in this study. However, the heat capacity data of this study have not been reported in the temperature range 910–1020 K. The enthalpy curve of Li_4SiO_4 is illustrated for the temperature interval 890–1040 K in Fig. 5. The standard deviation of a single experimental point is $\pm$ 3600 J mol^{-1} which is large compared to the integrals of the excess heat capacities δC_p. Therefore, quantitative results on the heat capacity are not given. The enthalpy curve is a continuous and differentiable function in this temperature range. The experimental results in the total temperature range are higher than the enthalpy and the heat capacity of Li_4SiO_4 estimated by Barin [15] which were obtained by application of the Neumann–Kopp rule to the constituent oxides.

Acknowledgements

The author gratefully acknowledges the supply of materials by Schott Glaswerke, Mainz, the experimental work by Mr. W. Laumer and the lattice parameter calculations by Dr. A. Skokan.

References

[1] A. Skokan, H. Wedemeyer, D. Vollath and E. Günther, Proc. 14th Symp. on Fusion Technology, Avignon, 1986, Pergamon Press, New York, 1986, p. 1255.
[2] A. Wittmann and E. Modern, Monatsh. Chem., 96 (1965) 581.
[3] H. Völlenkle, A. Wittmann and H. Novotny, Monatsh. Chem., 99 (1968) 1360.
[4] B.L. Dubey and A.R. West, J. Inorg. Nucl. Chem., 35 (1973) 3713.
[5] D. Tranqui, R.D. Shannon and H.Y. Chen, Acta Crystallogr. Sect. B, 35 (1979) 2479.
[6] G.W. Hollenberg, J. Nucl. Mater., 103–104 (1981) 591.
[7] A.R. West and F.P. Glasser, J. Mater. Sci., 5 (1970) 557.
[8] A.R. West and F.P. Glasser, J. Mater. Sci., 5 (1970) 676.
[9] W. Gratzer, H. Bittner, H. Novotny and K. Seifert, Z. Krist., 133 (1971) 260.
[10] E.I. Burmakin, G.V. Burov, I.G. Rosanov and G.K. Stepanov, Akad. Nauk SSSR, Uralskii Nauchn. Tsentr, 27 (1987) 64.
[11] D. Vollath and H. Wedemeyer, Adv. Ceram., 27 (1990) 3.
[12] R. Brandt and B. Schulz, J. Nucl. Mater., 152 (1988) 178.
[13] G.W. Hollenberg and D.E. Baker, HEDL-SA-2674-FP (1982).
[14] A. Asou, T. Terai and Y. Takahashi, J. Chem. Thermodyn., 24 (1992) 273.
[15] I. Barin, Thermochemical Data of Pure Substances, Verlag Chemie, Weinheim, 1989.
[16] R. Becker, Theorie der Wärme, 3rd edn., Springer-Verlag, Berlin, 1985.
[17] H. Moser, Physik. Z., 37 (1936) 737.
[18] R. Hultgren, P.R. Desai, D.T. Hawkins, M. Gleiser, K.K. Kelley and D.D. Wagman, Selected Values of the Thermodynamic Properties of the Elements and of Binary Alloys, ASM, Metals Park, 1973.
[19] E.F. Westrum, R.R. Walters, H.E. Flotow and D.W. Osborne, J. Chem. Phys., 48 (1968) 155.
[20] S.S. Todd and K.R. Bonnickson, J. Am. Chem. Soc., 73 (1951) 3894.
[21] B.A. Strukov, Soviet Phys., Solid State, 6 (1965) 2278.
[22] K. Ema, I. Hatta, K. Hamano and M. Tanaka, J. Phys. Soc. Jpn., 39 (1975) 1135.
[23] D.E. Mapother, Phys. Rev., 126 (1962) 2021.
[24] H. Kleykamp, Thermochim. Acta, 237 (1994) 1.
[25] S. Claus, H. Kleykamp and W. Smykatz-Kloss, J. Nucl. Mater., 230 (1996) 8.